



Published in final edited form as:

Nature. ; 485(7398): 327–332. doi:10.1038/nature10939.

Structure of the human kappa opioid receptor in complex with JD_Tic

Huixian Wu¹, Daniel Wacker¹, Vsevolod Katritch¹, Mauro Mileni¹, Gye Won Han¹, Eyal Vardy², Wei Liu¹, Aaron A. Thompson¹, Xi-Ping Huang², F. Ivy Carroll³, S. Wayne Mascarella³, Richard B. Westkaemper⁴, Philip D. Mosier⁴, Bryan L. Roth², Vadim Cherezov¹, and Raymond C. Stevens^{1,*}

¹Department of Molecular Biology, The Scripps Research Institute, 10550 North Torrey Pines Road, La Jolla, CA 92037, USA

²National Institute of Mental Health Psychoactive Drug Screening Program, Department of Pharmacology and Division of Chemical Biology and Medicinal Chemistry, University of North Carolina Chapel Hill Medical School, 4072 Genetic Medicine Building, Chapel Hill, NC 27514, USA

³Center for Organic and Medicinal Chemistry, Research Triangle Institute, P.O. Box 12194, Research Triangle Park, NC 27709, United States

⁴Department of Medicinal Chemistry, Virginia Commonwealth University, 800 E. Leigh Street, Richmond, VA 23298, USA

Abstract

Opioid receptors (ORs) mediate the actions of endogenous and exogenous opioids for many essential physiological processes including regulation of pain, respiratory drive, mood, and, in the case of κ -opioid receptors (KOR), dysphoria and psychotomimesis. Here we report the crystal structure of the human KOR (hKOR) in complex with the selective antagonist JD_Tic, arranged in

Users may view, print, copy, download and text and data- mine the content in such documents, for the purposes of academic research, subject always to the full Conditions of use: http://www.nature.com/authors/editorial_policies/license.html#terms

*To whom correspondence should be addressed: stevens@scripps.edu.

Supplementary Information is linked to the online version of the paper at www.nature.com/nature.

Author Contributions H.W. assisted protein expression, optimized the constructs, purified and crystallized the receptor in LCP, optimized crystallization conditions, grew crystals for data collection, collected the data and processed diffraction data, and prepared the manuscript. D.W. assisted with protein expression, purified the receptor, performed thermal stability assay and assisted with preparing the manuscript. V.K. performed nor-BNI/GNTI-receptor docking and prepared the manuscripts. M.M. assisted with protein expression, purified the receptor, tested the JD_Tic compound, and performed the thermal stability assay. G.W.H. solved and refined the structure and assisted with preparing the manuscript. E.V. created the initial tagged hKOR constructs and E.V. and X.-P.H. performed the ligand-binding and site-directed mutagenesis studies. W.L. assisted with construct optimization and crystallization in LCP. A.A.T. refined the structure and assisted with preparing the manuscript. F.I.C. and S.W.M. provided JD_Tic crystal structure, performed conformational studies of JD_Tic, and assisted with preparing the manuscript. R.B.W. and P.D.M. performed RB-64-receptor docking and prepared the manuscript. V.C. assisted with the crystallization in LCP, processed diffraction data, refined the structure and prepared the manuscript. B.L.R. suggested the JD_Tic compound for structural studies, supervised the pharmacology and mutagenesis studies and prepared the manuscript. R.C.S. was responsible for the overall project strategy and management and led the manuscript preparation and writing.

Author Information The coordinates and the structure factors have been deposited in the Protein Data Bank under the accession code (4DJH). Reprints and permissions information is available at www.nature.com/reprints. R.C.S. is a founder and BOD member of Receptos, a GPCR drug discovery company. Readers are welcome to comment on the online version of this article at www.nature.com/nature.

parallel-dimers, at 2.9 angstrom resolution. The structure reveals important features of the ligand binding pocket that contribute to JDtic's high affinity and subtype-selectivity for hKOR. Modeling of other important KOR-selective ligands, including the morphinan-derived antagonists nor-BNI and GNTI, and the diterpene agonist salvinorin A analog RB-64, reveals both common and distinct features for binding these diverse chemotypes. Analysis of site-directed mutagenesis and ligand structure-activity relationships confirms the interactions observed in the crystal structure, thereby providing a molecular explanation for hKOR subtype-selectivity along with insight essential for the design of hKOR compounds with new pharmacological properties.

The four opioid receptors (ORs), μ , δ , κ (MOR, DOR, KOR, and the nociceptin/orphanin FQ peptide receptor) belong to the class A (Rhodopsin-like) γ subfamily of G protein-coupled receptors (GPCRs)¹ with a common seven-transmembrane (7TM) helical architecture and are coupled predominantly to heterotrimeric G_i/G_o proteins; their activation by endogenous or exogenous ligands are linked to a number of neuropsychiatric sequelae including analgesia, sedation, depression, dysphoria, and euphoria². The three closely related subtypes, MOR, DOR and KOR, share ~70% sequence identity in their 7TM domains, with more variations in the extracellular loops (ECLs) and very little similarity in their N and C termini². The majority of endogenous opioid peptides have a defined preference to specific subtypes, for example, endorphins act via DORs and MORs, whereas dynorphins preferentially activate KORs. However, most exogenous and synthetic opioid ligands interact promiscuously (see K_i Database; <http://pdsp.med.unc.edu/pdsp.php>), likely due to the high degree of similarity of opioid-binding pockets. While decades of focused medicinal chemistry efforts have yielded reasonably selective ligands for all four ORs (see K_i Database), substantial interest continues for the development of subtype-selective agonists and antagonists.

Recent breakthroughs in elucidating high resolution structures of GPCRs in complex with small molecule³⁻⁷ and peptide⁸ ligands are providing details of their function⁹, leading to numerous rational ligand discovery studies^{10,11}. However, while most of these structures belong to the α subfamily of class A GPCRs¹, the highly diverse peptide-binding γ subfamily is represented only by the CXCR4 chemokine receptor⁸; additional structural coverage is needed to elucidate the repertoire of features¹² that define the pharmacological profile of the subfamily. KOR, identified based on studies with the κ -type prototypic agonist ketocyclazocine¹³, represents an attractive target for structure determination. Several KOR-selective partial agonists and antagonists have been developed as potential antidepressants, anxiolytics, and anti-addiction medications¹⁴, whereas a widely abused, naturally-occurring hallucinogen Salvinorin A (SaLA) was also found to be a highly selective KOR agonist¹⁵. Although many KOR agonists and antagonists have not demonstrated desirable pharmacological properties, lacking specificity or displaying frank psychotomimetic actions in humans^{14,16}, some have shown to be viable drug candidates. A KOR ligand in advanced stages of clinical development, JDtic, ((3*R*)-7-hydroxy-*N*-[(1*S*)-1-(((3*R*,4*R*)-4-(3-hydroxyphenyl)-3,4-dimethyl-1-piperidinyl)methyl)-2-methylpropyl]-1,2,3,4-tetrahydro-3-isoquinoline-carboxamide), was originally designed as a novel selective KOR antagonist¹⁷ that blocks the κ -agonist U50,488-induced antinociception, while not antagonizing μ -agonist induced analgesia¹⁸. JDtic also displays robust activity in rodent models of depression,

anxiety, stress-induced cocaine relapse, and nicotine withdrawal^{18,19}. Here, we report the crystal structure of a human KOR (hKOR) construct (hKOR-T4L) in complex with JD_{Tic} at 2.9 Å resolution. The results provide structural insights into the atomic details of molecular recognition and subtype-selectivity of KOR and related ORs, and should catalyze the structure-based design of advanced hKOR agonists and antagonists with improved pharmacological profiles and enhanced therapeutic efficacies.

Overall architecture of hKOR

Structural studies were carried out using an engineered hKOR construct (see Methods and Supplementary Fig. 1) and crystallized in cholesterol-doped monoolein lipidic cubic mesophase (see Methods). The construct used displayed pharmacological behavior similar to that of a native receptor expressed in HEK 293-T cells (Supplementary Tables 2 and 3). Data collection and refinement statistics are shown in Supplementary Table 1.

The structure of hKOR-JD_{Tic} was determined at 2.9 Å in the P 2₁2₁2₁ space group. The asymmetric unit (ASU) consists of a two receptors forming a parallel dimer (Fig. 1a). The dimer interface with ~1100 Å² buried surface area is formed through contacts between helices I, II and VIII (Fig. 1a, insert). Previously, parallel receptor dimers have been identified in crystal structures of activated rhodopsin (involving helices I, II and VIII)²⁰, β₂ adrenergic receptor (β₂AR; cholesterol mediated)³ and CXCR4 (involving helices IV, V and VI)⁸. Consistent with these crystallographic data, recent biochemical studies have suggested the existence of two dimerization interfaces: along helices IV and V - sensitive to receptor activation, and along helix I - insensitive to the state of activation²¹. While the orientations of the two T4-lysozyme (T4L) copies in the receptor monomers in one ASU differ by ~ 60° rotation, both copies of the receptor are highly similar (Fig. 1b) and will be treated identically except where otherwise noted. The remaining residues of the N- and C-termini in the hKOR/JD_{Tic} structure are disordered as in other class A GPCRs.

The main fold of the hKOR consists of a canonical 7TM bundle of α helices followed by an intracellular helix VIII that runs parallel to the membrane. (Fig. 1a, b), resembling previously solved GPCR structures^{3–8}. Structural comparison with other GPCRs suggests that hKOR has striking similarities in the ECL region with CXCR4, another peptide binding receptor in the γ subfamily. In the 7TM region, however, the hKOR structure is closer to aminergic receptors belonging to the α subfamily (RMSD_{Cα} ~2.3 Å for β₂AR, ~1.9 Å for Dopamine D3 receptor (D3R), and ~2.7 Å for CXCR4). The structure reveals distinctive features of hKOR, including: (i) conformation of the extracellular end of helix I that deviates from the position observed in CXCR4, where the tip of helix I is pulled towards the TM bundle by a disulfide bond between the N-terminus and ECL3. (ii) ECL2, the largest extracellular loop of hKOR, forms a β-hairpin similar to that observed in CXCR4, despite the low sequence similarity in this domain between the two receptors. Conservation of this feature between these peptide receptors suggests that the β-hairpin could be a common motif in the ECL2 of other γ subfamily receptors, where interactions between ECL2 and their endogenous peptide ligands are deemed important for ligand recognition and selectivity²². (iii) Unlike other solved non-rhodopsin class A GPCRs which have more than one disulfide bond, hKOR has only one formed between Cys131^{3,25} (superscripts indicate residue

numbering using the Ballesteros-Weinstein nomenclature²³) and Cys210, bridging ECL2 to the end of helix III. These two cysteines are conserved in all ORs and this disulfide bond is the canonical one shared by all other solved class A GPCRs. (iv) intracellular loop 2 (ICL2) adopts slightly different structures in the two hKOR molecules in the ASU, involving a two-turn α helix in molecule B, and only a one-turn α helix in molecule A (Supplementary Fig. 2), possibly reflecting the conformational plasticity of this region⁵. (v) ECL3 of hKOR is disordered. Of the approximately eleven residues in this loop (residues 300–310), six residues in molecule A and three in molecule B do not have interpretable electron density.

A common feature of the class A GPCRs is the presence of a conserved sequence motif Asp/Glu^{3.49}-Arg^{3.50}-Tyr^{3.51} (D/ERY) located at the cytoplasmic end of helix III. A salt bridge interaction between Arg^{3.50} and Asp/Glu^{6.30} from the cytoplasmic end of helix VI constitutes an “ionic lock”, which is thought to stabilize the inactive conformation of rhodopsin and other rhodopsin-like class A GPCRs^{5,24}, while its absence can enhance constitutive activity^{6,23}. Although hKOR lacks either of the acidic residues Asp/Glu at position 6.30, Arg156^{3.50} forms a hydrogen bond to another helix VI residue, Thr273^{6.34} (Supplementary Fig. 3a) in this inactive hKOR structure, thereby conceivably stabilizing the inactive receptor conformation. The NPxxY motif located at the cytoplasmic side of helix VII, which is composed of Asn326^{7.49}, Pro327^{7.50}, Ile328^{7.51}, Leu329^{7.52} and Tyr330^{7.53} in hKOR, is another highly conserved functional motif that is proposed to act as one of the molecular switches responsible for class A GPCR activation^{25,26}. Comparison of hKOR with inactive β_2 AR and A_{2A} adenosine receptor (A_{2A}AR) structures (Supplementary Fig. 3b) reveals a similar conformation of this motif in these receptors, thereby supporting the hypothesis that the observed hKOR-JDTic complex structure corresponds to the inactive state. To further establish that JDTic stabilizes an inactive conformation, we evaluated its ability to modulate G_i-mediated and β -arrestin-mediated signaling in transfected HEK293-T cells. We found that JDTic was devoid of agonist activity at both canonical and non-canonical pathways and completely blocked the effects of the prototypic agonist U69593 (Supplementary Fig. 4).

hKOR ligand binding pocket

The hKOR ligand binding pocket displays a unique combination of key characteristics both shared with and distinct from those in the chemokine and aminergic receptor families. While the hKOR binding pocket is comparatively large and partially capped by the ECL2 β -hairpin, as in CXCR4, it is also much narrower and deeper than in CXCR4 (Fig. 2c, d and Supplementary Fig. 5). In addition to a different set of side chains lining the pocket, the shape differences result from an approximately 4.5 Å inward shift of the extracellular tip of helix VI in hKOR as compared to CXCR4. The electron density clearly shows the position of the JDTic ligand (Supplementary Fig. 6), which reaches deep into the pocket to form ionic interactions with the Asp138^{3.32} side chain (Fig. 2a). The Asp^{3.32} residue is conserved in all aminergic GPCRs, thereby playing a critical role in the selectivity of aminergic receptors toward protonated amine-containing ligands. Asp^{3.32} is conserved in all ORs and for which modeling and mutagenesis studies²⁷ suggest an essential role in anchoring positively charged hKOR ligands.

Structural basis of JDtIc selectivity

JDtIc, developed as a derivative of the *trans*-(3*R*,4*R*)-dimethyl-4-(3-hydroxyphenyl) piperidine scaffold¹⁷, has exceptionally high affinity ($K_i = 0.32$ nM), potency ($K_i = 0.02$ nM in GTP γ S assays)^{17,28}, long duration of action and a more than 1000-fold selectivity for hKOR as compared to other OR subtypes¹⁸. Extensive structure–activity relationship (SAR) analyses performed on JDtIc analogues have yielded important insights into key determinants of JDtIc activity^{28–30}, although reliable identification of the interaction mode(s) and contact residues of these ligands has not been feasible without a receptor crystal structure.

The crystal structure of hKOR–JDtIc shows a tight fit of the ligand in the bottom of the binding cleft (Fig. 2a), forming ionic, polar, and extensive hydrophobic interactions with the receptor (Fig. 2b). The protonated amines in both piperidine and isoquinoline moieties of the ligand form salt bridges to the Asp138^{3,32} side chain (3.0 and 3.1 Å N–O distances, respectively). The piperidine amine is a part of the original *trans*-(3*R*,4*R*)-dimethyl-4-(3-hydroxyphenyl)piperidine scaffold, and is essential for binding³¹. SAR studies of JDtIc analogues show that the isoquinoline nitrogen can be replaced by carbon, oxygen or sulfur atoms with only ~10- to 50-fold reduction in affinity³⁰. Similar to the observed JDtIc conformation in the hKOR–JDtIc complex, a V-shaped conformation was found in the crystal structure of JDtIc by itself and which showed its amino groups coordinating a water molecule (Supplementary Fig. 7a). While several rotatable bonds within the JDtIc molecule allow for the sampling of different conformations (see Supplementary Fig. 7b) and facilitate the ligand passage through the narrow binding pocket entrance, the anchoring-type interaction of two amino groups with Asp138^{3,32} likely fixes the ligand in this characteristic V-shape.

SAR studies have also underscored the importance of the distal hydroxyl groups on both the piperidine and isoquinoline moieties of JDtIc, the removal of which did result in about a 100-fold reduction of affinity. A much smaller effect was observed upon methylation of these hydroxyls or their replacement by other polar groups²⁸. These SAR results suggest the importance of water-mediated interactions between these two hydroxyl groups and the receptor. Indeed, while the crystal structure does not show direct hydrogen bonding with the receptor for both hydroxyl groups, there is clear electron density for several structured water molecules that mediate their polar interactions (Supplementary Fig. 6).

The structure provides important clues for understanding the structural basis for the exceptional subtype selectivity of JDtIc. Among many extensive contacts, JDtIc interacts with four residues of the binding pocket that differ in other closely related ORs, which are thought to contribute to the subtype selectivity of JDtIc and other KOR-selective ligands³² (human MOR (hMOR) and human DOR (hDOR) amino acids shown in parentheses, respectively): Val108^{2,53} (Ala and Ala), Val118^{2,63} (Asn and Lys), Ile294^{6,55} (Val and Val), and Tyr312^{7,35} (Trp and Leu) (Fig. 2b and Supplementary Fig. 8). Analysis of JDtIc binding into hKOR-based hMOR and hDOR homology models, as well as JDtIc SAR results^{17,28,30} (Supplementary Fig. 9), suggest that all described residues can contribute to the JDtIc selectivity profile. Thus, changes in the Val118^{2,63} side chain, where larger

hydrophilic residues, Asn^{2.63} and Lys^{2.63} are found in hMOR and hDOR, respectively, are likely to introduce unfavorable contacts with JD_{Tic}. Additionally, changing Tyr312^{7.35} to the Trp^{7.35} and Leu^{7.35} residues found in hMOR and hDOR, respectively, are likely to result in the loss of an important polar interaction with the JD_{Tic} amide. The remaining two hydrophobic side chains replacements, Val to Ala at position 2.53 and Ile to Val at position 6.55, may cause a reduction of the hydrophobic contact between JD_{Tic} and the receptor.

The isopropyl group from JD_{Tic} reaches deep in the orthosteric pocket to form a hydrophobic interaction with a conserved Trp287^{6.48} side chain (aka the “rotamer toggle switch”), possibly playing a critical role in the pharmacological properties of this ligand. Trp^{6.48} is thought to be a key part of the activation mechanism in many class A GPCRs including rhodopsin²⁶ and A_{2A}AR²⁵, and similar hydrophobic contacts have been implicated in blocking activation-related conformational changes in the dark state visual rhodopsin by 11-*cis* retinal, and by inverse agonists in the A_{2A}AR and D3R.

Binding of KOR-selective morphinans

Prior mutagenesis and modeling studies suggested that many small molecule opioid ligands can interact with KOR, as well as with MOR and DOR, by forming a salt bridge with the highly conserved Asp^{3.32} (ref^{33,34}). This is consistent with our mutagenesis studies (Supplementary Table 3) and flexible docking³⁵ of a series of morphine analogues, including selective KOR antagonists nor-BNI and GNTI (Fig. 3 and Supplementary Fig. 10). To assess the compatibility of these bulky and rigid ligands with the observed hKOR protein backbone conformation, we performed global energy optimizations of nor-BNI and GNTI in the binding cavity of hKOR, keeping side chains of the binding pocket fully flexible. Multiple independent runs consistently resulted in low energy conformations with essentially identical poses and receptor contacts for the common naltrexone moieties of both nor-BNI and GNTI (RMSD = 0.85 Å). In addition to a highly complementary van der Waals interface, both compounds formed an amino group salt bridge to the Asp138^{3.32} side chain and a hydrogen bond to the Tyr139^{3.33} side chain, both of which are important anchoring points for binding of morphine-based ligand, as supported by previous mutagenesis studies³⁴.

Moreover, unlike JD_{Tic}, both nor-BNI and GNTI compounds have a second basic moiety located more than 10 Å away from the first amino group (the other morphine in nor-BNI and the guanidine moiety in GNTI). In the predicted models of hKOR- nor-BNI/GNTI complexes, these additional amino groups of both ligands form a salt bridge with Glu297^{6.58} located at the entrance to the ligand binding pocket, which was previously characterized as a residue critical for subtype selectivity of hKOR-selective morphinan derivatives³⁶. This interaction is also supported by our mutagenesis results (Supplementary Table 3), where a Glu297Ala mutation induced a significant drop in both nor-BNI and GNTI binding, but did not affect JD_{Tic} binding. Hydrophobic interactions at the KOR-specific residue Ile294 were also found for both nor-BNI and GNTI; consistent with our mutagenesis results (Supplementary Table 3) and suggesting that Ile294 may also be important for developing KOR subtype selective morphinan derivatives. Additional polar interactions with hKOR-specific residues, Glu209 and Ser211 in ECL2, are found for nor-BNI, which may further

enhance hKOR-selectivity of this bulky ligand. Another side chain of the pocket, His291^{6.52}, which is involved in the highly conserved aromatic cluster around Trp^{6.48} and thought to play a critical role in the receptor activation process³⁷, forms hydrophobic contacts with JD_{Tic}, nor-BNI and GNTI. His291^{6.52} can be mutated to another aromatic residue, phenylalanine, without disrupting binding of these antagonists (Supplementary Table 3). The non-conservative His291^{6.52}Lys mutation, however, totally abolished binding of all tested ligands, likely because of the disruption of the aromatic cluster induced by the lysine side chain. Interestingly, the cyclopropyl moiety of both nor-BNI and GNTI in these binding poses has the same position as the isopropyl moiety of JD_{Tic}, making hydrophobic contact with the conserved residue Trp287^{6.48}. This cyclopropyl moiety is generally implicated in conversion of opioid agonists into antagonists (e.g. agonist oxycodone into antagonist naltrexone), and this effect may be partially explained by a direct interaction with the Trp287^{6.48} side chain.

Overall, these structure-based docking results support the ‘message-address’ model³⁸ in applications to morphine-based ligands nor-BNI and GNTI³⁶, which points to Glu297^{6.58} as a key side chain that controls hKOR selectivity by anchoring the ‘address’ moieties of these compounds. The crystal structure of hKOR-JD_{Tic} complex (Fig. 2 and 3), however demonstrates that even in lieu of “address” interaction with Glu297^{6.58} more than 1000-fold subtype-selectivity to hKOR can be achieved for JD_{Tic} and some of its derivatives. Importantly, then, the ‘message-address’ hypothesis does not uniformly apply to all hKOR-selective antagonists.

Binding of Salvinorins

Salvinorin A (SaLA), a naturally occurring diterpene from the widely abused hallucinogenic plant *Salvia divinorum*, represents an exceedingly potent ($EC_{50} = 1$ nM) and selective KOR agonist (>1000-fold)¹⁵. SaLA is unique compared to other KOR ligands in that it lacks a charged or polar nitrogen atom to anchor it in the binding pocket. Extensive site-directed mutagenesis, SCAM (substituted cysteine-accessibility mutagenesis) and SAR studies on SaLA and its analogues have been performed, indicating (among others) that the 2-acetoxy moiety interacts with Cys315^{7.38} (ref³⁹). Possible modes of interaction between the cysteine-reactive and ultra-potent agonist and SaLA analog 22-thiocyanatosalvinorin A (RB-64; $K_i = 0.59$ nM; $EC_{50} = 0.077$ nM)³⁹, and the hKOR structure were thus evaluated. Exposure of hKOR to RB-64 produces irreversibly-bound, wash-resistant adducts that are tethered to Cys315^{7.38} (ref³⁹). As the thiocyanate group contains two electrophilic centers, two distinct adducts may be formed, increasing the mass by either 463 or 431 amu. Docking studies using GOLD⁴⁰ predict that the salvinorin 2-position can access Cys315^{7.38} while maintaining many of the interactions implicated by site-directed mutagenesis for SaLA, providing a possible mechanism for the formation of the KOR–RB-64 adduct (Fig. 4, Supplementary Tables 4–5 and Figs. 11–12). Additionally, the docking results serve as a model of the initial recognition process of SaLA-related agonists of the hKOR in an inactive state, although additional studies will be needed to fully elucidate the nature of the SaLA-induced activation mechanism.

Conclusions

The JD_{Tic}-hKOR crystal structure has uncovered a combination of key features shared with chemokine and aminergic GPCRs along with unique structural details characteristic of the opioid subfamily. The hKOR was crystallized as a parallel-dimer with contacts involving helices I, II and VIII. While the existence of GPCR dimers *in vivo* and their physiological relevance remain highly debatable, several distinct potential dimer interfaces are starting to emerge from crystallographic and biochemical studies. Such multiple dimerization interfaces may serve to support different functional pathways, as well as to promote oligomeric assembly of GPCRs. Analysis of the ligand-receptor interactions has revealed important molecular details responsible for the exceptionally high affinity and subtype selectivity of JD_{Tic}—a small molecule antagonist with a broad therapeutic potential. The elucidation of a large binding cavity with a multitude of potential anchoring points begins to explain both the extreme structural diversity of hKOR drugs and differences in their receptor interaction modes, as supported by differential effects of various site-directed mutations on the binding properties of chemically diverse prototypic ligands. The structure clearly provides a long anticipated molecular framework for understanding opioid drug action, and thereby affords valuable new opportunities for a structure-based discovery of new drugs with ideal pharmacological properties.

Methods Summary

hKOR-T4L was expressed in *Spodoptera frugiperda* (*Sf9*) cells. Ligand-binding and functional assays were performed as described in Methods. *Sf9* cells were solubilized using 1% (w/v) *n*-dodecyl- β -D-maltopyranoside (DDM) and 0.2% (w/v) cholesteryl hemisuccinate (CHS), and purified by immobilized metal ion affinity chromatography (IMAC), followed by reverse IMAC after cleaving N-terminal FLAG-10xHis tags by His-tagged Tobacco Etch Virus (TEV) protease. The purified protein was mixed with monoolein and cholesterol in a ratio of 40%:54%:6% (w/w) to form lipidic cubic phase (LCP) from which the receptor was crystallized. Crystals were grown at 20 °C in 45 nl protein-laden LCP boluses overlaid by 800 nl of precipitant solutions as described in Methods. Crystals were harvested from the LCP matrix and flash frozen in liquid nitrogen. X-ray diffraction data were collected on the 23ID-B/D beamline (GM/CA CAT) at the Advanced Photon Source, Argonne, IL using a 10 μ m minibeam at wavelength of 1.0330 Å. Data collection, processing, structure solution and refinement are described in Methods. Modeling of JD_{Tic} analogues and hKOR-selective morphine derivatives nor-BNI and GNTI was performed using ICM-Pro; SYBYL-X 1.3 and GOLD Suite 5.1 were used to model RB-64 complexes, as described in Methods.

Full Methods and any associated references are available in the online version of the paper at www.nature.com/nature.

Supplementary Material

Refer to Web version on PubMed Central for supplementary material.

Acknowledgments

This work was supported by PSI:Biography grant U54 GM094618 (R.C.S.) for biological studies and structure production, NIH Roadmap grant P50 GM073197 (R.C.S.) for technology development and R01 DA017624 (B.L.R., E.V., R.B.M., P.D.M.), R01 DA027170 (B.L.R.), the NIMH Psychoactive Drug Screening Program Contract (B.L.R., X.-P.H.), the Michael Hooker Distinguished Chair of Pharmacology (B.L.R.), and the NIH grant R01 DA009045 (F.I.C.). D.W. is supported by a Boehringer Ingelheim Fonds Ph.D. Fellowship. The JDTC X-ray structure was conducted by Laboratory for the Structure of Matter, Naval Research Laboratory, Washington, DC. We thank J. Velasquez for help on molecular biology; T. Trinh, K. Allin and M. Chu for help on baculovirus expression; V. Setola for help with functional activity assays; J. Evans for help acquiring compounds; the National Institute of Drug Abuse Drug Supply Program for supplying JDTC and other opioid ligands used in these studies; K. Kadyshchanskaya for assistance with figure preparation; E. Abola for assistance with manuscript preparation; A. Walker for assistance with manuscript preparation; J. Smith, R. Fishetti, and N. Sanishvili for assistance in development and use of the minibeam and beamtime at GM/CA-CAT beamline 23-ID at the Advanced Photon Source, which is supported by National Cancer Institute grant Y1-CO-1020 and National Institute of General Medical Sciences grant Y1-GM-1104.

Literature Cited

1. Fredriksson R, Lagerstrom MC, Lundin LG, Schiöth HB. The G-protein-coupled receptors in the human genome form five main families. Phylogenetic analysis, paralogon groups, and fingerprints. *Mol Pharmacol*. 2003; 63:1256–1272. [PubMed: 12761335]
2. Waldhoer M, Bartlett SE, Whistler JL. Opioid receptors. *Annu Rev Biochem*. 2004; 73:953–990. [PubMed: 15189164]
3. Cherezov V, et al. High-resolution crystal structure of an engineered human beta2-adrenergic G protein-coupled receptor. *Science*. 2007; 318:1258–1265. [PubMed: 17962520]
4. Jaakola VP, et al. The 2.6 angstrom crystal structure of a human A2A adenosine receptor bound to an antagonist. *Science*. 2008; 322:1211–1217. [PubMed: 18832607]
5. Chien EY, et al. Structure of the human dopamine D3 receptor in complex with a D2/D3 selective antagonist. *Science*. 2010; 330:1091–1095. [PubMed: 21097933]
6. Warne T, et al. Structure of a beta1-adrenergic G-protein-coupled receptor. *Nature*. 2008; 454:486–491. [PubMed: 18594507]
7. Shimamura T, et al. Structure of the human histamine H1 receptor complex with doxepin. *Nature*. 2011; 475:65–70. [PubMed: 21697825]
8. Wu B, et al. Structures of the CXCR4 chemokine GPCR with small-molecule and cyclic peptide antagonists. *Science*. 2010; 330:1066–1071. [PubMed: 20929726]
9. Rasmussen SG, et al. Crystal structure of the beta2 adrenergic receptor-Gs protein complex. *Nature*. 2011; 477:549–555. [PubMed: 21772288]
10. Katritch V, Cherezov V, Stevens RC. Diversity and modularity of G protein-coupled receptor structures. *Trends Pharmacol Sci*. 2011
11. Congreve M, Langmead CJ, Mason JS, Marshall FH. Progress in structure based drug design for G protein-coupled receptors. *J Med Chem*. 2011; 54:4283–4311. [PubMed: 21615150]
12. Kufareva I, Rueda M, Katritch V, Stevens RC, Abagyan R. Status of GPCR modeling and docking as reflected by community-wide GPCR Dock 2010 assessment. *Structure*. 2011; 19:1108–1126. [PubMed: 21827947]
13. Martin WR, Eades CG, Thompson JA, Huppler RE, Gilbert PE. The effects of morphine- and nalorphine- like drugs in the nondependent and morphine-dependent chronic spinal dog. *J Pharmacol Exp Ther*. 1976; 197:517–532. [PubMed: 945347]
14. Carlezon WA Jr, Beguin C, Knoll AT, Cohen BM. Kappa-opioid ligands in the study and treatment of mood disorders. *Pharmacol Ther*. 2009; 123:334–343. [PubMed: 19497337]
15. Roth BL, et al. Salvinorin A: a potent naturally occurring nonnitrogenous kappa opioid selective agonist. *Proc Natl Acad Sci U S A*. 2002; 99:11934–11939. [PubMed: 12192085]
16. Walsh SL, Strain EC, Abreu ME, Bigelow GE. Enadoline, a selective kappa opioid agonist: comparison with butorphanol and hydromorphone in humans. *Psychopharmacology (Berl)*. 2001; 157:151–162. [PubMed: 11594439]

17. Thomas JB, et al. Identification of the first trans-(3R,4R)- dimethyl-4-(3-hydroxyphenyl)piperidine derivative to possess highly potent and selective opioid kappa receptor antagonist activity. *J Med Chem.* 2001; 44:2687–2690. [PubMed: 11495579]
18. Carroll I, et al. Pharmacological properties of JDtic: a novel kappa-opioid receptor antagonist. *Eur J Pharmacol.* 2004; 501:111–119. [PubMed: 15464069]
19. Jackson KJ, Carroll FI, Negus SS, Damaj MI. Effect of the selective kappa-opioid receptor antagonist JDtic on nicotine antinociception, reward, and withdrawal in the mouse. *Psychopharmacology (Berl).* 2010; 210:285–294. [PubMed: 20232057]
20. Salom D, et al. Crystal structure of a photoactivated deprotonated intermediate of rhodopsin. *Proc Natl Acad Sci U S A.* 2006; 103:16123–16128. [PubMed: 17060607]
21. Mancia F, Assur Z, Herman AG, Siegel R, Hendrickson WA. Ligand sensitivity in dimeric associations of the serotonin 5HT_{2c} receptor. *EMBO Rep.* 2008; 9:363–369. [PubMed: 18344975]
22. Wang JB, Johnson PS, Wu JM, Wang WF, Uhl GR. Human kappa opiate receptor second extracellular loop elevates dynorphin's affinity for human mu/kappa chimeras. *J Biol Chem.* 1994; 269:25966–25969. [PubMed: 7929306]
23. Ballesteros JA, Weinstein H. Integrated methods for the construction of three-dimensional models and computational probing of structure-function relations in G protein-coupled receptors. *Methods Neurosci.* 1995; 25:366–428.
24. Palczewski K, et al. Crystal structure of rhodopsin: A G protein-coupled receptor. *Science.* 2000; 289:739–745. [PubMed: 10926528]
25. Xu F, et al. Structure of an Agonist-Bound Human A_{2A} Adenosine Receptor. *Science.* 2011; 332:322–327. [PubMed: 21393508]
26. Standfuss J, et al. The structural basis of agonist-induced activation in constitutively active rhodopsin. *Nature.* 2011; 471:656–660. [PubMed: 21389983]
27. Subramanian G, Paterlini MG, Larson DL, Portoghese PS, Ferguson DM. Conformational analysis and automated receptor docking of selective arylacetamide-based kappa-opioid agonists. *J Med Chem.* 1998; 41:4777–4789. [PubMed: 9822548]
28. Cai TB, et al. Synthesis and in vitro opioid receptor functional antagonism of analogues of the selective kappa opioid receptor antagonist (3R)-7-hydroxy-N-((1S)-1-[[[(3R,4R)-4-(3-hydroxyphenyl)-3,4-dimethyl-1-piperidinyl]methyl]-2-methylpropyl]-1,2,3,4-tetrahydro-3-isoquinolinecarboxamide (JDtic). *J Med Chem.* 2008; 51:1849–1860. [PubMed: 18307295]
29. Thomas JB, et al. Importance of phenolic address groups in opioid kappa receptor selective antagonists. *J Med Chem.* 2004; 47:1070–1073. [PubMed: 14761209]
30. Runyon SP, et al. Analogues of (3R)-7-hydroxy-N-[(1S)-1-[[[(3R,4R)-4-(3-hydroxyphenyl)-3,4-dimethyl-1-piperidinyl]methyl]-2-methylpropyl]-1,2,3,4-tetrahydro-3-isoquinolinecarboxamide (JDtic). Synthesis and in vitro and in vivo opioid receptor antagonist activity. *J Med Chem.* 2010; 53:5290–5301. [PubMed: 20568781]
31. Zimmerman DM, Nickander R, Horng JS, Wong DT. New structural concepts for narcotic antagonists defined in a 4-phenylpiperidine series. *Nature.* 1978; 275:332–334. [PubMed: 692714]
32. Vortherms TA, Mosier PD, Westkaemper RB, Roth BL. Differential helical orientations among related G protein-coupled receptors provide a novel mechanism for selectivity. Studies with salvinorin A and the kappa-opioid receptor. *J Biol Chem.* 2007; 282:3146–3156. [PubMed: 17121830]
33. Surratt CK, et al. -mu opiate receptor. Charged transmembrane domain amino acids are critical for agonist recognition and intrinsic activity. *J Biol Chem.* 1994; 269:20548–20553. [PubMed: 8051154]
34. Befort K, et al. The conserved aspartate residue in the third putative transmembrane domain of the delta-opioid receptor is not the anionic counterpart for cationic opiate binding but is a constituent of the receptor binding site. *Mol Pharmacol.* 1996; 49:216–223. [PubMed: 8632752]
35. Totrov M, Abagyan R. Flexible protein-ligand docking by global energy optimization in internal coordinates. *Proteins Suppl.* 1997; 1:215–220.
36. Metzger TG, Paterlini MG, Portoghese PS, Ferguson DM. Application of the message-address concept to the docking of naltrexone and selective naltrexone-derived opioid antagonists into opioid receptor models. *Neurochem Res.* 1996; 21:1287–1294. [PubMed: 8947918]

37. Chen S, et al. Mutation of a single TMVI residue, Phe(282), in the beta(2)-adrenergic receptor results in structurally distinct activated receptor conformations. *Biochemistry*. 2002; 41:6045–6053. [PubMed: 11993999]
38. Chavkin C, Goldstein A. Specific receptor for the opioid peptide dynorphin: structure--activity relationships. *Proc Natl Acad Sci U S A*. 1981; 78:6543–6547. [PubMed: 6118865]
39. Yan F, et al. Structure-based design, synthesis, and biochemical and pharmacological characterization of novel salvinorin A analogues as active state probes of the kappa-opioid receptor. *Biochemistry*. 2009; 48:6898–6908. [PubMed: 19555087]
40. Verdonk ML, Cole JC, Hartshorn M, Murray CW, Taylor R. Improved Protein-Ligand Docking Using GOLD. *Proteins*. 2003; 52:609–623. [PubMed: 12910460]
41. Rosenbaum DM, et al. GPCR engineering yields high-resolution structural insights into beta2-adrenergic receptor function. *Science*. 2007; 318:1266–1273. [PubMed: 17962519]
42. Caffrey M, Cherezov V. Crystallizing membrane proteins using lipidic mesophases. *Nat Protoc*. 2009; 4:706–731. [PubMed: 19390528]
43. Cherezov V, Peddi A, Muthusubramaniam L, Zheng YF, Caffrey M. A robotic system for crystallizing membrane and soluble proteins in lipidic mesophases. *Acta Crystallogr D Biol Crystallogr*. 2004; 60:1795–1807. [PubMed: 15388926]
44. Cherezov V, et al. Rastering strategy for screening and centring of microcrystal samples of human membrane proteins with a sub-10 microm size X-ray synchrotron beam. *J R Soc Interface*. 2009; 6 (Suppl 5):S587–597. [PubMed: 19535414]
45. Otwinowski Z, Minor W. Processing of X-ray diffraction data collected in oscillation mode. *Method Enzymol*. 1997; 276:307–326.
46. McCoy AJ, et al. Phaser crystallographic software. *J Appl Crystallogr*. 2007; 40:658–674. [PubMed: 19461840]
47. Murshudov GN, Vagin AA, Dodson EJ. Refinement of macromolecular structures by the maximum-likelihood method. *Acta Crystallogr D Biol Crystallogr*. 1997; 53:240–255. [PubMed: 15299926]
48. BUSTER. Vol. 2.8.0. Global Phasing Ltd; Cambridge, U.K: 2009.
49. Emsley P, Lohkamp B, Scott WG, Cowtan K. Features and development of Coot. *Acta Crystallogr D Biol Crystallogr*. 2010; 66:486–501. [PubMed: 20383002]

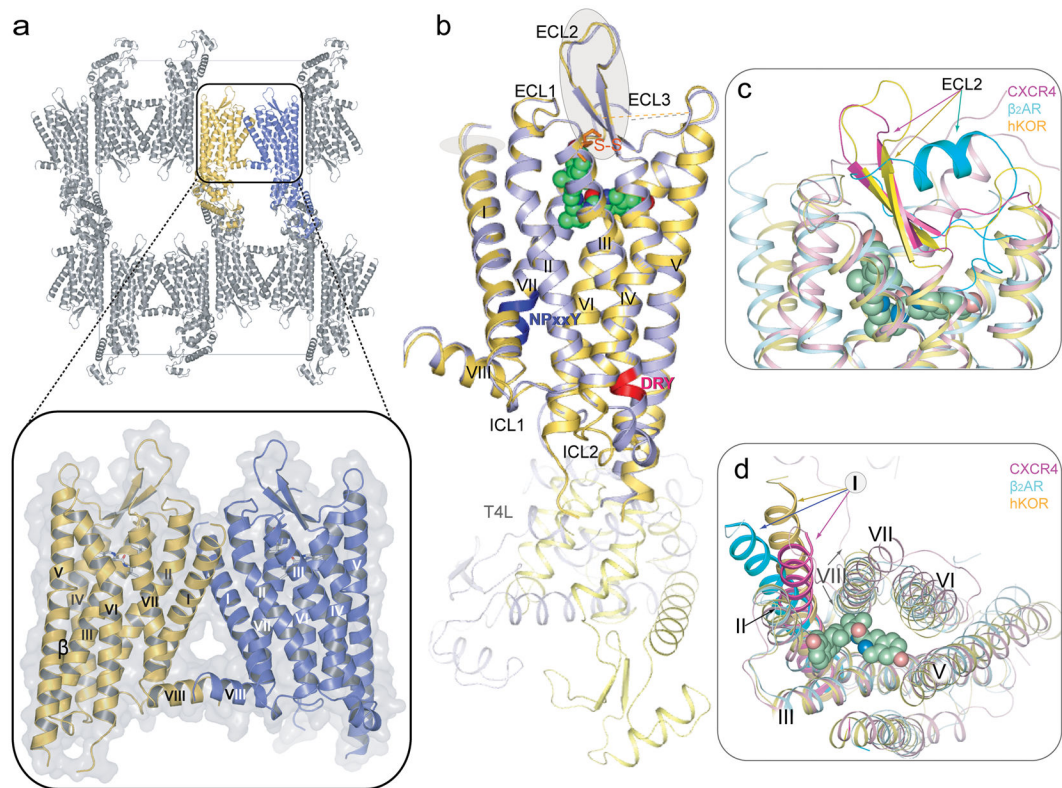


Figure 1. Crystal packing and overview of the hKOR structure in complex with JDtic, and comparison with the inactive CXCR4 and β_2 AR structures
(a) hKOR-T4L crystal packing. The parallel-dimer in one ASU is highlighted by insert. **(b)** Overall architecture of hKOR-T4L in complex with JDtic. A molecule (yellow) and B molecule (blue) in one ASU are aligned through the receptor part. The DRY and NPxxY motifs are highlighted in red and blue, respectively. JDtic is shown in a green sphere representation and the disulfide bonds are colored orange. **(c)** Side and **(d)** extracellular views of a structural alignment of hKOR (yellow); CXCR4 (PDB ID: 3ODU; magenta) and β_2 AR (PDB ID: 2RH1; cyan). The graphics were created by PyMOL.

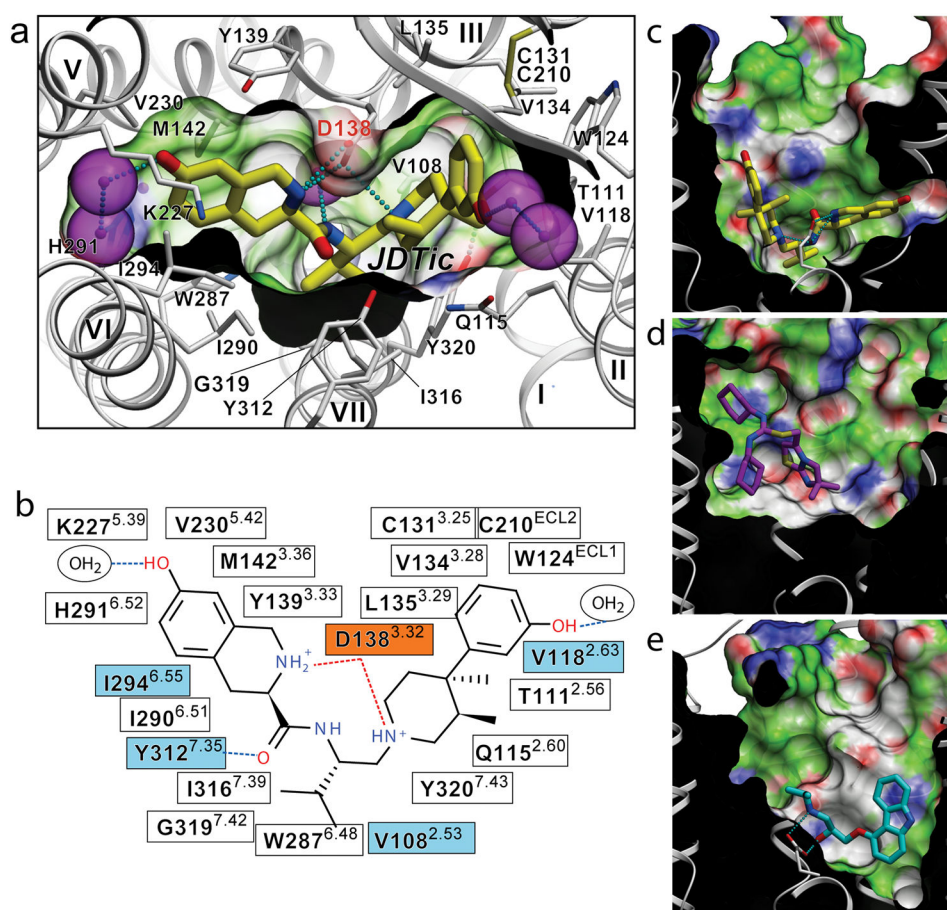


Figure 2. Binding of the high affinity selective antagonist JDtic in the hKOR crystal structure (a) Conformation of the binding pocket with JDtic shown by sticks with yellow carbons. The protein is displayed in cartoon representation looking down from the extracellular side, with the 22 contact residues within 4.5 Å from the ligand shown by white sticks. The pocket surface is shown as a semitransparent surface colored according to binding properties (green: hydrophobic, blue: H-bond donor, red: H-bond acceptor). Salt bridges and hydrogen bonds are shown as dotted lines. Structured water molecules are shown as large magenta spheres. (b) Diagram of ligand interactions in the binding pocket side chains at 4.5 Å cutoff. Salt bridges are shown in red and direct hydrogen bonds in blue dashed lines. Ballesteros-Weinstein numbering is shown as superscript. Residues that vary among MOR, DOR and KOR subtypes are highlighted in cyan, and residue Asp138^{3.32} inferred in hKOR ligand binding by mutagenesis data, is highlighted orange. Side views of the sliced binding pocket in (c) hKOR-JDtic, (d) CXCR4-IT1t, and (e) β_2 AR-carazolol complexes. The pocket surfaces are colored as in panel A, the protein interior is black and the extracellular space is white. Ligands are shown as capped sticks with carbons colored yellow (JDtic), magenta (IT1t) and cyan (carazolol). Asp^{3.32} side chains in hKOR-JDtic and β_2 AR-carazolol complexes are shown by thin sticks with grey carbons. The graphics were prepared using ICM molecular modeling package (Molsoft LLC).

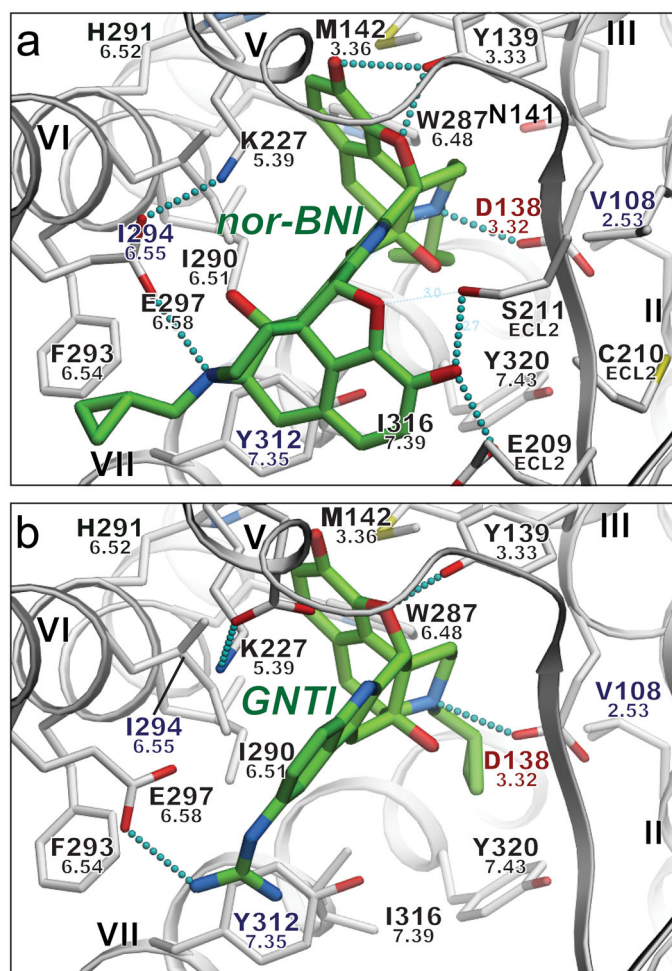


Figure 3. Putative interaction modes of morphine-based high affinity hKOR selective antagonists nor-BNI (a) and GNTI (b)

Ligands are depicted as capped sticks with green carbons, and contact side chains of the receptor within 4 Å from the ligand are shown with grey carbons. Key hydrogen bonds and salt bridges are indicated with small cyan spheres and residues unique to KOR are labeled in blue. Residue Asp138^{3,32}, which also shows critical impact on GNTI and nor-BNI binding in mutagenesis studies, is highlighted red. Ballesteros-Weinstein residue numbers are shown under the hKOR residue numbers. The graphics were prepared using ICM molecular modeling package (Molsoft LLC).

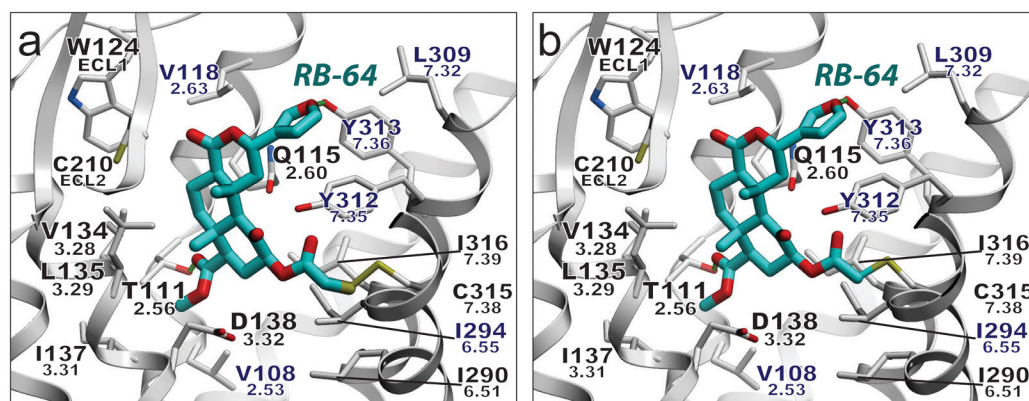


Figure 4. Model of covalently-bound RB-64

Putative binding mode of (a) the RB-64 +463 amu and (b) the RB-64 +431 amu adduct.

Residues within 4 Å of the ligand are displayed. Rendering: ligand, capped sticks/cyan carbons; hKOR side chains, capped sticks; hydrogen bonds, small green spheres; hKOR-unique residues labeled in blue. Ballesteros-Weinstein residue numbers are shown under the hKOR residue numbers. The graphics were prepared using ICM molecular modeling package (Molsoft LLC).